

Speeding up deep neural network-based planning of local car maneuvers via efficient B-spline path construction

Piotr Kicki and Piotr Skrzypczyński

Abstract—This paper demonstrates how an efficient representation of the planned path using B-splines, and a construction procedure that takes advantage of the neural network’s inductive bias, speed up both the inference and training of a DNN-based motion planner. We build upon our recent work on learning local car maneuvers from past experience using a DNN architecture, introducing a novel B-spline path construction method, making it possible to generate local maneuvers in almost constant time of about 11 ms, respecting a number of constraints imposed by the environment map and the kinematics of a car-like vehicle. We evaluate thoroughly the new planner employing the recent Bench-MR framework to obtain quantitative results showing that our method outperforms state-of-the-art planners by a large margin in the considered task.

I. INTRODUCTION

Although autonomous vehicles are researched intensively, research on motion planning for these vehicles focuses mostly on managing traffic scenarios and rules [1], [2], paying less attention to the local maneuvers that are necessary to park a car in a crowded city center, to enter a shopping mall’s garage, or to avoid a collision with another car that executes an unexpected maneuver. Human drivers perform such local maneuvers intuitively, leveraging the experience from similar situations they have encountered in the past. Unlike humans, planning algorithms still struggle to produce feasible paths in a very short time (usually fractions of seconds) avoiding collisions in dangerous situations, and satisfying the constraints of a car-like vehicle. A car is non-holonomic, has a limited steering angle and some physical dimensions, while the planned path should allow control with continuous velocity and acceleration due to safety and comfort considerations. Although these requirements call for a solution that is rather a reactive behavior than a classic planning algorithm, reactive methods [3] rarely produce smooth paths for the highly constrained scenarios we consider because of the vulnerability to local minima and the use of hard-coded heuristics.

Here machine learning comes to the rescue, as modern methods, like deep neural networks (DNN), make it possible to learn even complicated decision-making policies in constrained state spaces [4]. We have explored this idea in our recent paper [5], where we presented a neural network architecture and a training procedure that allow a local motion planner to learn from its own experience (Fig. 1). The neural network is trained with the use of a deep reinforcement learning framework, using gradient-based policy search [6].

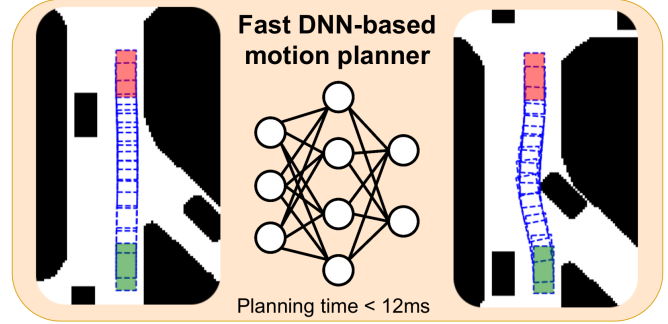


Fig. 1. Motivational example of a traffic situation that requires rapid path planning in order to handle safely the unexpected maneuver of another road user (here the car coming from the right side)

Learning through the interaction seems to carry out the most important information to improve the performance of the trained system [7], while it does not impose any upper-bounds on it, unlike supervised learning, which performance is bounded by the quality of the reference trajectories or human demonstrations.

Although our previously introduced DNN [5] keeps the path computation time below 50 ms, some emergency maneuvers require even faster replanning, at the sensor frame rate of at least 30 fps, still yielding smooth paths satisfying all the constraints. Therefore, we contribute in this paper a novel path parametrization and procedure of its construction, which enables our method to compute yet better paths in an even shorter time in comparison to [5]¹. The new parametrization, even though it follows the idea of the approximation of an implicitly defined oracle planning function, breaks up with the Markov Decision Process formalism used in [5], instead plans the whole maneuver at once. The path is no longer represented with a sequence of polynomials, but with a single 7th degree B-spline curve. The new representation and the matching architecture of the DNN guarantee that the planned path reaches the goal configuration accurately, unlike the previous solution that usually produced small offsets. The proposed path construction procedure introduces an inductive bias [8] to the DNN, which significantly speeds up the training.

We evaluate thoroughly the new planning method using the latest motion planning benchmarking software Bench-MR [9], which allows us to demonstrate that our solution is superior to both state-of-the-art planners and the solution from [5] in the considered task of local maneuver generation.

Authors are with Institute of Robotics and Machine Intelligence, Poznan University of Technology, ul. Piotrowo 3A, 60-965 Poznan, Poland
name.surname@put.poznan.pl

¹Implementation of the proposed planner and code used for the experiments can be found at https://github.com/pkicki/neural_path_planning/tree/bspline.

II. RELATED WORK

The problem of motion planning for vehicles has been tackled multiple times in the literature with a broad spectrum of algorithms following different paradigms, such as graph search [10], sampling-based planning [11], trajectory optimization [12], [13] or probabilistic motion primitives [14]. For the last two decades, sampling-based algorithms are considered the group of methods most suitable to efficiently plan paths in complicated configuration spaces. Extensions of the Rapidly-exploring Random Trees (RRT) concept allow asymptotically optimal planning [11], while more recent algorithms, such as Batch Informed Trees (BIT*) [15] or Adaptively Informed Trees (AIT*) [16] quickly find a feasible path, and if the computational time permits, converge towards the optimal one. Unfortunately, few of the sampling-based algorithms intrinsically consider the constraints of a kinematic car [17]. Fast path planning respecting the non-holonomic constraints is possible using for example the State Lattices algorithm [18], but requires motion primitives with 0 curvature at the boundaries to preserve the curvature continuity. Using the continuous curvature Dubins curves [19] (cc-Dubins) with some sampling-based algorithm leads to the paths that achieve unnecessarily high curvatures. Hence, the planning results, even if computed as quickly as from our DNN, are not equivalent to our smooth paths that can be easily followed by a standard controller [20].

Only a few of the planning algorithms utilize the experience gained in the tasks executed before or some easily accessible *a priori* knowledge in order to improve future planning attempts. This concept is relatively new in robotics [21], [22], however in a way innate and natural for humans, as we all use the experience gathered throughout life to improve our future actions. Most of the works in this field consider ways to improve the speed of sampling-based motion planners by biasing the sampling distribution [23] or directly predicting the next node [24]. The concept of teaching neural networks how to plan has been applied in several recent papers [7], [25], [26], however, all of those approaches have considered only a reaching problem for manipulators. The use of deep reinforcement learning for motion planning in autonomous vehicles in a context wider than path planning is surveyed in the recent paper [27]. Among the works that leverage neural networks for vehicle path planning [28] uses DNN and data collected from human drivers to learn a driving policy in urban scenarios, while [29] deals with local maneuvers with an end-to-end approach that casts the task of selecting the steering angle as a classification problem. Recently, Xiao *et al.* [30] introduced the novel Learning from Hallucination technique to address vehicle motion planning in highly constrained spaces. A jointly learnable behavior and trajectory planner for self-driving vehicles was introduced in [31]. Unlike the majority of neural planning methods that rely on paths demonstrated by experts, we apply a deep reinforcement learning approach [4], thus conserving both the time and human effort in the training phase.

III. NEURAL NETWORK LOCAL PATHS GENERATION

A. Problem definition

In order to focus the presented research on a concrete problem of practical value, we define the task of planning a feasible monotonic, curvature-continuous path \mathcal{P} from an initial state q_0 to the desired state q_d , taking into account the geometry of the vehicle (modeled with a rectangle), the local environment (a grid map of the size $25.6\text{ m} \times 25.6\text{ m}$ represented with resolution 0.2 m), and typical kinematic constraints of an Ackermann steering car (no lateral and longitudinal slip, and limited steering angle β).

B. Proposed solution

We observe that different path planning methods, although they are algorithms, can be viewed as mappings from some problem's space to the space of the solution. Thus, we can consider a special type of such a mapping, that for all elements of some set of motion planning problems returns a single feasible path that solves the given problem instance. We have introduced functions which have this property as *oracle planning functions* in [5]. It is hardly possible to define explicitly such a function for a broad set of practical planning problems. However, knowing the properties of such a function we can define it implicitly for a specified problem, by introducing the constraints and quality criteria imposed on its output. Because of this, we propose an oracle planning function approximator, which tries to mimic the oracle planning function behavior by being optimized to produce motion plans that satisfy the constraints and maximize the quality criteria.

We propose to train a neural network how to plan feasible paths that solve the instances of the introduced problem i.e. how to approximate the oracle planning function. This neural network takes as input a map of the environment together with initial q and desired q_d vehicle configurations, processes these data, and returns a representation of the path. We use a neural network which is a further development of the architecture proposed in [5], but its final processing block (the parameters estimator) is changed, in order to take advantage of the novel representation of the generated path (see Fig. 2) we introduce here. The new way the resultant path is constructed makes it possible to generate the final path from a single neural network prediction. This, in turn, enables the new method to plan extremely fast and to produce paths that are smoother and have a warranty of reaching the goal. Furthermore, the new architecture introduces some important inductive bias to the neural network, which speeds up its training significantly.

C. Path representation

In contrast to [5], we propose here to represent the solution path with a 7th degree B-spline curve [32]. This representation allows us to define a path, parametrized by its length, that starts and ends at given positions, with certain orientation and initial curvature, thus we can ensure that the boundary constraints imposed by the given planning problem

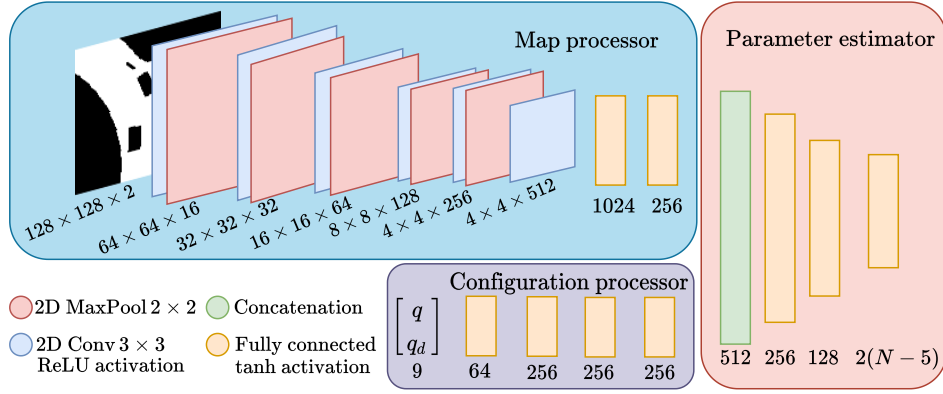


Fig. 2. Architecture of the proposed neural network with the parameter estimator for B-spline-based paths

are satisfied. The new B-spline representation is essential for allowing the neural network to generate the path in a single inference, making the planning process very fast.

D. Neural network based path generation

To define a 7th degree B-spline one has to provide control points $p_i = (x_i, y_i) \in \mathbb{R}^2$ for $i = 0, 1, \dots, N-1$. While 5 of them (the first 3 and the last 2) are defined already by the boundary conditions of the planning problem, the rest have to be determined by the neural network. Unfortunately, allowing the neural network to simply produce some control points on the map does not work. A randomly initialized neural network produces a bunch of control points randomly placed around the center of the map, which results in an extremely tangled curve that intersects with itself and is hard to entangle taking into account the curvature constraints.

Therefore, considering the task of planning local maneuvers for a car-like vehicle, we propose to organize the neural network predictions in a binary tree-like structure to produce paths without self-intersections. Each control point p_i is determined with the use of another two adjacent control points (p_j, p_k) that are already in the tree, such that a neural network prediction is scaled to fit in the square, with a side length of $d_{j,k} = \max\{|x_j - x_k|, |y_j - y_k|\}$, centered in the middle of those points. Thus, the resultant position of the control point p_i can be defined by

$$p_i = \frac{p_j + p_k}{2} + \frac{1}{2}d_{j,k} \cdot (\phi_{2(i-3)}, \phi_{2(i-3)+1}), \quad (1)$$

where $(\phi_{2(i-3)}, \phi_{2(i-3)+1}) \in [-1; 1]^2$ are two predictions made by a neural network.

The tree of control points, is built starting from the root p_{2+2^D-1} , where D is the tree depth. To define the root of the tree p_{2+2^D-1} , the p_2 and p_{N-2} boundary control points, and two neural network predictions $(\phi_{2(2^D-1)-1}, \phi_{2(2^D-1)-1+1})$ are used (because of two-dimensional control points). Next, points at the second level $p_{2+2^{D-2}}, p_{2+2^{D-1}+2^{D-2}}$ are defined. They have to lie in between root and the boundary control points, therefore they are determined using analogue elements of the neural network output and the pairs of control points p_2, p_{2+2^D-1} and $p_{2+2^{D-1}}, p_{N-2}$. Similarly, the next tree level can be populated with another 4 control

points, using corresponding neural network outputs and all points which are already in the tree, together with the aforementioned boundary control points p_2 and p_{N-2} . In the same way, the next 8 points can be added in between the control points of the previous tree level. The idea of the proposed path generation procedure, for $D = 2$, is described graphically in Figure 3.

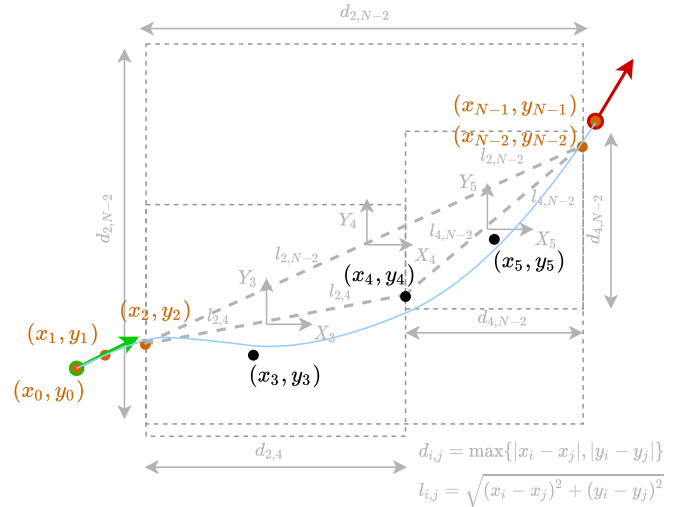


Fig. 3. General idea of defining the B-spline control points. Brown control points are stemming from the motion planning problem boundary conditions, while black ones are determined by the neural network output and two adjacent control points which defines the area where the new point can be placed

Such a way of constructing the path from the neural network outputs is beneficial in terms of the feasibility of the training process and introduces an inductive bias into the inference and learning phase. Due to this representation, the neural network, even randomly initialized, favors paths that have smaller curvature, do not self-intersect, and are ensured to connect initial and goal configurations. To fit this representation, we proposed the neural network architecture presented in Figure 2. Its outputs are in the range $[-1; 1]$ due to the use of the \tanh function, and are interpreted as x and y coordinates of the control points in the coordinate systems determined by their parents in the tree.

E. Differentiable loss function

To train this neural network, we utilize the idea of the implicitly defined *oracle planning function* and formulate a loss function:

$$\mathcal{L} = \mathcal{L}_{curv} + \mathcal{L}_{coll} + \sigma_{tcurv} \gamma \mathcal{L}_{tcurv}, \quad (2)$$

where \mathcal{L}_{curv} is a loss that penalizes paths that violate the curvature constraints, \mathcal{L}_{coll} penalizes paths that are not collision-free, whereas the $\gamma \mathcal{L}_{tcurv}$ term minimizes the sum of changes in curvature along the path, but only if the indicator function $\sigma_{tcurv} = 1$, i.e. when other loss terms are zeroing out. Such a construction of the loss function stimulates the oracle planning function approximator to produce paths that have the same properties as the oracle planning function ($\mathcal{L}_{curv} = \mathcal{L}_{coll} = 0$), and are characterized by reduced changes in the steering angle β along the path due to the total curvature loss \mathcal{L}_{tcurv} scaled with the parameter γ , which in our experiments was set to 0.1.

While all components of the loss function (2) are inspired by the ones introduced in [5], we redefined the way how the \mathcal{L}_{curv} and \mathcal{L}_{tcurv} losses are calculated and used almost the same procedure for the collision loss \mathcal{L}_{coll} .

Due to the B-spline representation, we are able to easily obtain the first and second derivatives of the generated path using its control points, instead of relying on the local approximations, as it was done in [5]. Therefore, to calculate the curvature κ of the path, we sample the 1024 equally distant points on the B-splines of its first and second derivatives, and obtain 1024 samples of the curvature $\kappa_0, \kappa_1, \dots, \kappa_{1023}$. Using these samples we can define the curvature loss \mathcal{L}_{curv} by

$$\mathcal{L}_{curv} = \sum_{i=0}^{1023} \max(|\kappa_i| - \kappa_{max}, 0), \quad (3)$$

where $\kappa_{max} = \frac{1}{R_{min}}$ is the maximum allowed path curvature, that stems from the vehicle minimal turning radius R_{min} . Whereas, total curvature loss \mathcal{L}_{tcurv} is defined by

$$\mathcal{L}_{tcurv} = \sum_{i=1}^{1023} |\kappa_i - \kappa_{i-1}|, \quad (4)$$

while collision loss \mathcal{L}_{coll} is defined by

$$\mathcal{L}_{coll} = \sum_{i=1}^{1023} \sigma_{coll}(\Pi_i, \mathcal{F}) \sum_{k=0}^4 d(\mathcal{P}_r, \Pi_{ik}) l_i, \quad (5)$$

where σ_{coll} is the collision indicator function, which is equal to 1 if any part of the vehicle circumference Π_i at i -th point on a curve lies outside the free space \mathcal{F} , $d(\mathcal{P}_r, \Pi_{ik})$ is the Euclidean distance between the k -th characteristic point (4 corners of the rectangular body of the vehicle and the guiding point in the middle of the rear axle) and the reference path \mathcal{P}_r , whereas l_i is the Euclidean distance between i -th and $(i-1)$ -th points on a path. Notice that the auxiliary reference path is used during learning only to evaluate the \mathcal{L}_{coll} component of the loss function, suggesting how to retreat from the collision areas. As we do not evaluate the similarity between this path, and the learned

one, the auxiliary path does not give an upper bound for the performance of our algorithm. Whereas the reference path can be produced by any planning method for nonholonomic, car-like vehicles, we use State Lattices [18], mostly because of its simplicity and speed.

Importantly, all considered losses are differentiable with respect to the neural network outputs and thus the gradient of the proposed loss function can be used to directly optimize the neural network weights using gradient descend algorithms.

IV. EXPERIMENTAL EVALUATION

To evaluate the proposed B-spline neural network planner, we trained it for 400 epochs with a learning rate $5 \cdot 10^{-4}$ and batch size 128 on the training dataset introduced in [5], which consists of more than 130000 scenarios on 23517 local maps obtained from both simulated and real missions of autonomous cars. We used the same model of a car as in [5], with maximal admissible curvature $\kappa_{max} = 0.227 \text{ m}^{-1}$, length equal to 4.05 m and width of 1.72 m. For the training NVIDIA GTX1080Ti GPU was used, while for inference an IntelCore i7-9750H CPU was sufficient to obtain the required planning times.

Firstly, we analyzed the dependency of the neural network-based motion planner from the depth of the control points tree D . Results of this experiment are presented in Figure 4. One can see, that by increasing the depth of the tree, the running time grows, mainly because there is more time needed to interpret the neural network predictions as the number of control points grows exponentially with D . However, in the case of the accuracy of the models (understood as the ratio of feasible plans generated by the neural network to the overall number of the problems in the test set), the dependency is much less trivial. Accuracy, as expected, grows with the number of control points but only till the $D = 3$, after which it decreases slightly. This phenomenon can be explained by the fixed capacity of the neural network, which may be not able to determine so many control points, and the fact that for problems that require a relatively short solution path it is

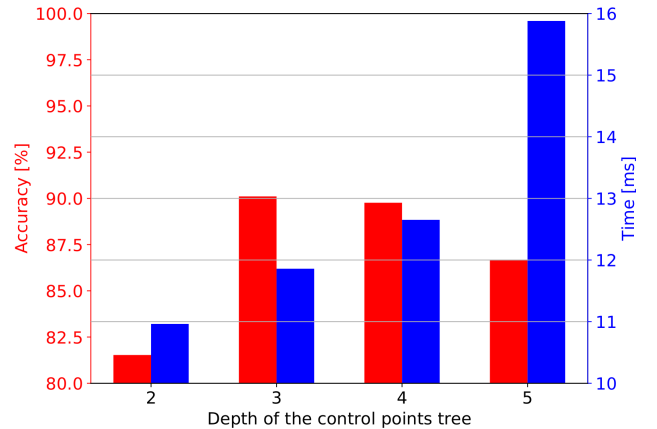


Fig. 4. Accuracy and inference time with respect to the depth of the control points tree D . Model with $D = 3$ achieves the best accuracy with reasonable low computational effort

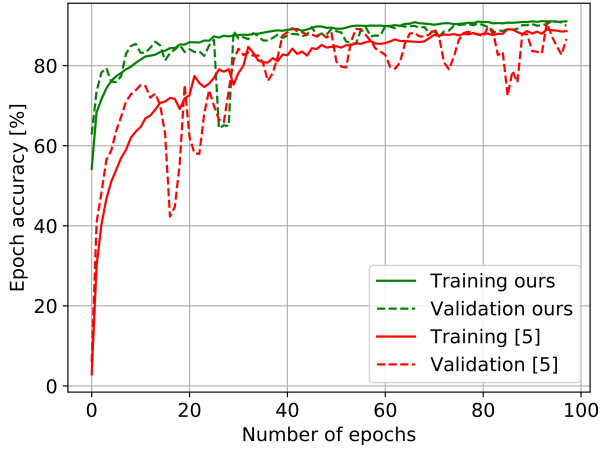


Fig. 5. Accuracy on the training and validation sets obtained by the neural network planner proposed in this paper and in [5] throughout the learning process

hard to fit all control points, such that the resultant path does not violate the curvature constraints. Taking into account obtained results, we decided to use a neural network model with $D = 3$ for further experiments.

Then, we analyzed the learning curve of the proposed model for $D = 3$ in comparison with the model from [5]. In Figure 5 one can see the revealed inductive bias of the introduced representation, which enables the proposed neural network to achieve about 60% accuracy on the validation set just after the first epoch of training and about 80% after the 10th epoch.

Figure 6 shows exemplary paths generated with the use of the proposed B-spline neural network planner for the scenarios not included in the training set. Moreover, we present the generalization abilities of the proposed solution, by visualizing the sets of final configurations for which our model was able to generate a feasible path.

Table I presents a numerical comparison of the proposed B-spline motion planning network with other path planning methods for a car-like vehicle with curvature constraints. This comparison was done on the test part of the dataset introduced in [5], with the use of planners from the motion planning benchmark Bench-MR [9] adapted to interface with the motion planning problems from [5]. This adoption required only to implement an interface to properly import the grid maps from our dataset and to make minor changes in the vehicle model. We believe that this approach, together with the open-source code of our planner, makes the presented results easily repeatable, and allows others to compare with our proposal.

The first method which we considered was the State Lattice algorithm, implemented in the SBPL library [33], which was operating on the grid with 0.2 m spatial and $\frac{\pi}{16}$ rad angular resolution. It was equipped with 11 different motion primitives per orientation, which were made with 3rd order B-splines with 0 curvature at the boundaries to preserve the continuity of the path curvature. The second algorithm was the BIT* [15] equipped with continuous curvature Dubins

curves [19]. We limited its running time to 100 ms to achieve a comparable time scale. While we tested other sampling-based motion planning algorithms available in the Bench-MR framework, such as SORRT* [34] and InformedRRT* [35], their accuracy was about 20% (even for maximal allowed planning time equal to 1 s), thus we chose only BIT* for the comparison. Next baselines are the two versions of the neural motion planner introduced in [5]. The model directly taken from [5] is denoted NMP I, whereas in the case of the model named NMP II we reduced 10 times the allowed deviation between the desired and the actually reached configurations. Thus, NMP II shows how introducing more tight constraints on the final configuration impacts the performance.

We can see that only the NMP I model achieved better accuracy than the one proposed in this paper. However, it is important to notice, that this model is allowed to finish the path in a subset of configurations around the goal, and as we can see in the case of NMP II, reduction of the size of this subset leads to degradation of the performance. Even lower accuracy was achieved by the SL and BIT* algorithms, which suggests that these methods are unable to plan in such a short time for more complicated scenarios. Significantly better accuracy was achieved by the B-spline neural network planner (about 90%), which also noted the lowest mean planning time equal to 11 ms (on i7 CPU) that is almost constant for all test scenarios. What is more, the proposed planning method produces paths that are the smoothest ones, have the lowest mean of the maximal curvature (κ), and are free from some tedious constraints such as zeroing the curvature at the ends of every segment (SL) or generating paths with high maximal curvature (BIT*).

TABLE I

ACCURACY, PLANNING TIME, AVERAGE MAXIMAL CURVATURE OF THE PATH, AND ITS ORDER OF CONTINUITY FOR FOLLOWING PLANNING METHODS: STATE LATTICES [33], [9] (SL), BIT* WITH CONTINUOUS CURVATURE DUBINS CURVES [15], [9], NEURAL MOTION PLANNER [5] (NMP I/II) AND THE SOLUTION PROPOSED IN THIS PAPER (OURS).

Planner	SL	BIT*	NMP I	NMP II	ours
Accuracy [%]	49.4	72.83	92.24	79.25	90.1
Time [ms]	23±27	45±35	43±2	43±2	11±1
Mean max κ [m^{-1}]	0.179	0.226	0.152	0.192	0.145
Continuity	\mathbb{G}^2	\mathbb{G}^2	\mathbb{G}^2	\mathbb{G}^2	\mathbb{G}^5

In Figures 7 and 8 we present the performance of the proposed planner in comparison to BIT* (with Dubins and cc-Dubins extenders) on some relatively hard motion planning problems, each of which requires precise maneuvers in a confined space. For all considered problems our planner was able to plan a collision-free path, that satisfies the curvature constraints within 12 ms, in contrast to the BIT* with continuous curvature Dubins paths, that was unable to do so, even when run for 100 s. The reason it performs so poorly may be due to problems with sampling states that are possible to connect with cc-Dubins curves, and the need of including the clothoid segments between the straight lines and arcs, which is hard to perform when

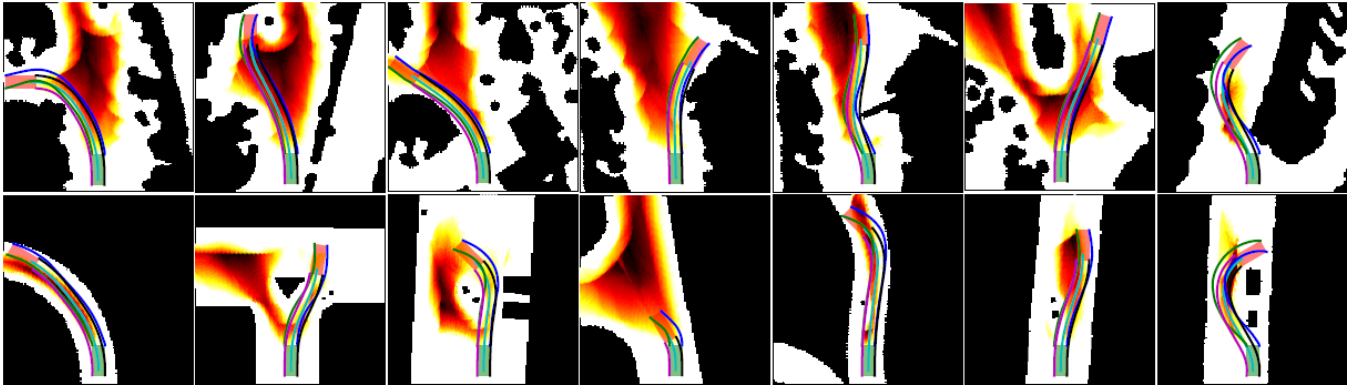


Fig. 6. Visualizations of the reachable sets (presented as heatmaps: darker areas are reachable with greater orientations ranges) and sample paths generated by the proposed B-spline neural network motion planner on the maps unseen in the training process

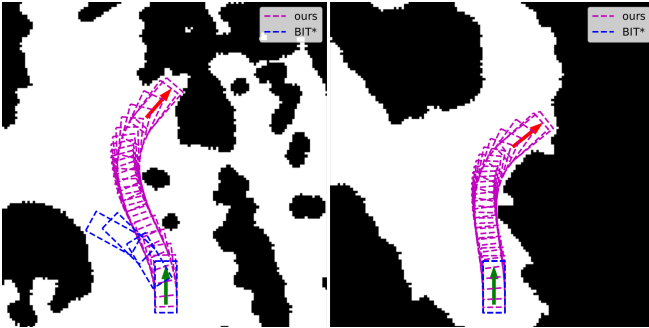


Fig. 7. Paths generated by the proposed planner (purple) and BIT* with continuous curvature Dubins curves (blue) for two different motion planning problems which may be considered hard

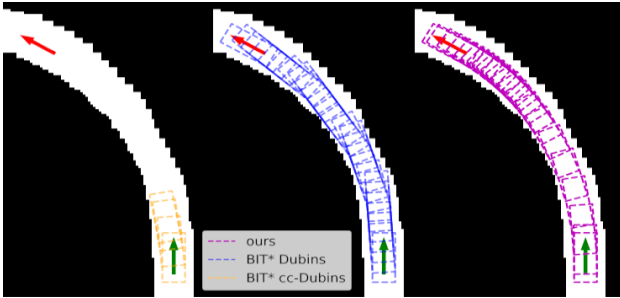


Fig. 8. Paths generated by the proposed planner (purple) and BIT* with continuous curvature Dubins curves (orange) and BIT* with plain Dubins curves (blue) for the turn scenario on the extremely narrow road

there is not enough space. To validate if resigning from the path curvature continuity will ease the planning process, we checked the BIT* algorithm with typical Dubins paths on a narrow turn. Results of this comparison are shown in Figure 8. One can see, that using cc-Dubins paths makes it impossible to complete the maneuver, whereas plain Dubins curves reach the goal state, but collide with the environment in the narrowest part of the maneuver. This type of maneuver exposes the problems in planning with the use of curves which enables to plan fast, but at the same time imposes severe constraints on the curvature of path segments. In contrast, the proposed solution is able to plan extremely fast, while being able to produce smooth paths with a curvature tailored to the specific task.

V. CONCLUSIONS

We presented an important improvement to the DNN-based approach to local maneuver generation for self-driving cars introduced in [5], that reduces the planning time to about 11 ms, ensures that the generated path reaches the desired configuration accurately, and increases the order of path continuity. The new architecture of our DNN introduces also an inductive bias due to the way the resultant path is constructed. As result, the neural network is trained much faster than the previous one and achieves about 60% accuracy just after the 1st epoch.

The conducted evaluation shows that the proposed method achieves 90.1% accuracy on the test set outperforming other planning algorithms such as State Lattices and BIT*, as well as the neural motion planner from [5] for the reduced set of allowed final configurations. Moreover, our novel algorithm generates paths with the lowest mean of maximal curvatures for the considered scenarios, which allows for higher velocities or smaller centrifugal forces. The proposed B-spline neural motion planner generalizes to the previously unseen maps and scenarios and can handle typical local maneuvers, such as parking, sharp turns, avoiding obstacles, or navigating in narrow passages. We have demonstrated in [5] by CARLA simulations that our neural planner can handle dynamic environments. The new approach should improve also on this aspect, due to the even shorter planning time. However, considering dynamic environments directly by prediction of the occupied areas from the time sequence of local maps is in our agenda for future work. Moreover, future work concerns the possibility to use our path generator as an initial guess for optimization-based motion planners, which can help to achieve higher accuracy in an acceptable time. We are also working on the integration of the new planner with the CARLA simulation environment, as we did in the previous version, which, however, requires a substantial change in the path following controller.

REFERENCES

- [1] A. Artunedo, J. Villagra, and J. Godoy, "Real-time motion planning approach for automated driving in urban environments," *IEEE Access*, vol. 7, pp. 180 039–180 053, 2019.

- [2] L. Claussmann, M. Revilloud, D. Gruyer, and S. Glaser, "A review of motion planning for highway autonomous driving," *IEEE Transactions on Intelligent Transportation Systems*, vol. 21, no. 5, pp. 1826–1848, 2020.
- [3] P. Qu, J. Xue, L. Ma, and C. Ma, "A constrained VFH algorithm for motion planning of autonomous vehicles," in *IEEE Intelligent Vehicles Symposium (IV)*, 2015, pp. 700–705.
- [4] H. Sun, W. Zhang, R. Yu, and Y. Zhang, "Motion planning for mobile robots focusing on deep reinforcement learning: A systematic review," *IEEE Access*, vol. 9, pp. 69 061–69 081, 2021.
- [5] P. Kicki, T. Gawron, K. Ćwian, M. Ozay, and P. Skrzypczyński, "Learning from experience for rapid generation of local car maneuvers," *Engineering Applications of Artificial Intelligence*, vol. 105, p. 104399, 2021.
- [6] M. P. Deisenroth, G. Neumann, and J. Peters, "A survey on policy search for robotics," *Foundations and Trends in Robotics*, vol. 2, no. 1–2, pp. 1–141, 2013.
- [7] J. Jurgenson and T. Aviv, "Harnessing reinforcement learning for neural motion planning," in *Robotics: Science and Systems*, Freiburg, 2019.
- [8] M. Hessel, H. van Hasselt, J. Modayil, and D. Silver, "On inductive biases in deep reinforcement learning," 2019.
- [9] E. Heiden, L. Palmieri, L. Bruns, K. O. Arras, G. S. Sukhatme, and S. Koenig, "Bench-MR: A motion planning benchmark for wheeled mobile robots," *IEEE Robotics and Automation Letters*, vol. 6, no. 3, pp. 4536–4543, 2021.
- [10] D. Dolgov, S. Thrun, M. Montemerlo, and J. Diebel, "Path planning for autonomous driving in unknown environments," in *Experimental Robotics*, ser. STAR, vol. 54. Springer, 2009, pp. 55–64.
- [11] S. Karaman and E. Frazzoli, "Sampling-based algorithms for optimal motion planning," *The International Journal of Robotics Research*, vol. 30, no. 7, pp. 846–894, 2011.
- [12] A. Arab, K. Yu, J. Yi, and D. Song, "Motion planning for aggressive autonomous vehicle maneuvers," in *IEEE International Conference on Automation Science and Engineering*, 2016, pp. 221–226.
- [13] C. Rösmann, F. Hoffmann, and T. Bertram, "Kinodynamic trajectory optimization and control for car-like robots," in *IEEE/RSJ International Conference on Intelligent Robots and Systems (IROS)*, 2017, pp. 5681–5686.
- [14] T. Löw, T. Bandyopadhyay, J. Williams, and P. V. K. Borges, "PROMPT: probabilistic motion primitives based trajectory planning," in *Robotics: Science and Systems XVII, Virtual Event, July 12-16, 2021*, 2021.
- [15] J. D. Gammell, T. D. Barfoot, and S. S. Srinivasa, "Batch informed trees (BIT*): Informed asymptotically optimal anytime search," *The International Journal of Robotics Research*, vol. 39, no. 5, pp. 543–567, 2020.
- [16] M. P. Strub and J. D. Gammell, "Adaptively informed trees (AIT*): Fast asymptotically optimal path planning through adaptive heuristics," pp. 3191–3198, 2020.
- [17] J. L. Blanco, M. Bellone, and A. Gimenez-Fernandez, "TP-Space RRT – kinematic path planning of non-holonomic any-shape vehicles," *International Journal of Advanced Robotic Systems*, vol. 12, no. 5, p. 55, 2015.
- [18] M. Pivtoraiko, R. A. Knepper, and A. Kelly, "Differentially constrained mobile robot motion planning in state lattices," *Journal of Field Robot.*, vol. 26, no. 3, pp. 308–333, 2009.
- [19] T. Fraichard and A. Scheuer, "From Reeds and Shepp's to continuous-curvature paths," *IEEE Transactions on Robotics*, vol. 20, no. 6, pp. 1025–1035, 2004.
- [20] M. M. Michałek and T. Gawron, "VFO path following control with guarantees of positionally constrained transients for unicycle-like robots with constrained control input," *Journal of Intelligent & Robotic Systems*, vol. 89, no. 1, pp. 191–210, 2018.
- [21] D. Berenson, P. Abbeel, and K. Goldberg, "A robot path planning framework that learns from experience," in *IEEE International Conference on Robotics and Automation*, Saint Paul, 2012, pp. 3671–3678.
- [22] N. Jetchev and M. Toussaint, "Fast motion planning from experience: trajectory prediction for speeding up movement generation," *Autonomous Robots*, vol. 34, no. 1, pp. 1573–7527, 2013.
- [23] B. Ichter, J. Harrison, and M. Pavone, "Learning sampling distributions for robot motion planning," in *IEEE International Conference on Robotics and Automation (ICRA)*, 2018, pp. 7087–7094.
- [24] A. H. Qureshi, A. Simeonov, M. J. Bency, and M. C. Yip, "Motion planning networks," in *IEEE International Conference on Robotics and Automation*, 2019, pp. 2118–2124.
- [25] M. J. Bency, A. H. Qureshi, and M. C. Yip, "Neural path planning: Fixed time, near-optimal path generation via oracle imitation," in *IEEE/RSJ International Conference on Intelligent Robots and Systems (IROS)*, 2019, pp. 3965–3972.
- [26] A. H. Qureshi, Y. Miao, A. Simeonov, and M. C. Yip, "Motion planning networks: Bridging the gap between learning-based and classical motion planners," *IEEE Transactions on Robotics*, vol. 37, no. 1, pp. 48–66, 2021.
- [27] S. Aradi, "Survey of deep reinforcement learning for motion planning of autonomous vehicles," *IEEE Transactions on Intelligent Transportation Systems*, pp. 1–20, 2020.
- [28] J. Chen, B. Yuan, and M. Tomizuka, "Deep imitation learning for autonomous driving in generic urban scenarios with enhanced safety," in *IEEE/RSJ International Conference on Intelligent Robots and Systems*, 2019, pp. 2884–2890.
- [29] M. Q. Dao, D. Lanza, and V. Frimont, "End-to-end deep neural network design for short-term path planning," in *11th IROS Workshop on Planning, Perception, Navigation for Intelligent Vehicle (PPNIV 2019)*, Macau, 2019.
- [30] X. Xiao, B. Liu, G. Warnell, and P. Stone, "Toward agile maneuvers in highly constrained spaces: Learning from hallucination," *IEEE Robotics and Automation Letters*, vol. 6, no. 2, pp. 1503–1510, 2021.
- [31] A. Sadat, M. Ren, A. Pokrovsky, Y. Lin, E. Yumer, and R. Urtasun, "Jointly learnable behavior and trajectory planning for self-driving vehicles," in *IEEE/RSJ International Conference on Intelligent Robots and Systems*, 2019, pp. 3949–3956.
- [32] C. de Boor, *A Practical Guide to Splines*. New York: Springer Verlag, 1978.
- [33] M. Likhachev and D. Ferguson, "Planning long dynamically feasible maneuvers for autonomous vehicles," *The International Journal of Robotics Research*, vol. 28, no. 8, pp. 933–945, 2009.
- [34] I. A. Sucan, M. Moll, and L. E. Kavraki, "The open motion planning library," *IEEE Robotics & Automation Magazine*, vol. 19, no. 4, pp. 72–82, 2012.
- [35] J. D. Gammell, T. D. Barfoot, and S. S. Srinivasa, "Informed sampling for asymptotically optimal path planning," *IEEE Transactions on Robotics*, vol. 34, no. 4, pp. 966–984, 2018.